



Concurrent assessment of gait kinematics using marker-based and markerless motion capture

Robert M. Kanko ^{a,*}, Elise K. Laende ^a, Elysia M. Davis ^a, W. Scott Selbie ^b, Kevin J. Deluzio ^a

^a Mechanical and Materials Engineering, Queen's University, Canada

^b Theia Markerless Inc, Kingston, Canada



ARTICLE INFO

Keywords:

Markerless motion capture
Gait analysis
Kinematics
Deep learning

ABSTRACT

Kinematic analysis is a useful and widespread tool used in research and clinical biomechanics for the quantification of human movement. Common marker-based optical motion capture systems are time intensive and require highly trained operators to obtain kinematic data. Markerless motion capture systems offer an alternative method for the measurement of kinematic data with several practical benefits. This work compared the kinematics of human gait measured using a deep learning algorithm-based markerless motion capture system to those from a standard marker-based motion capture system. Thirty healthy adult participants walked on a treadmill while data were simultaneously recorded using eight video cameras and seven infrared optical motion capture cameras, providing synchronized markerless and marker-based data for comparison. The average root mean square distance (RMSD) between corresponding joint centers was less than 2.5 cm for all joints except the hip, which was 3.6 cm. Lower limb segment angles relative to the global coordinate system indicated the global segment pose estimates from both systems were very similar, with RMSD of less than 5.5° for all segment angles except those that represent rotations about the long axis of the segment. Lower limb joint angles captured similar patterns for flexion/extension at all joints, ab/adduction at the knee and hip, and toe-in/toe-out at the ankle. These findings indicate that the markerless system would be a suitable alternative technology in cases where the practical benefits of markerless data collection are preferred.

1. Introduction

Kinematic analysis is the measurement of the motion of rigid bodies and is an important tool in clinical and research biomechanics. While kinematic analyses are ubiquitous in biomechanics research, the experimental and computational methods used to estimate three-dimensional (3D) segment position and orientation (pose) vary, and so do the resulting kinematics. Markerless motion capture has the potential to alleviate some of the technical and practical issues of marker-based motion analysis by replacing physical palpation and skin surface marker tracking of bony landmarks with probabilistic estimation of landmark positions using trained neural networks (Mathis et al., 2018).

Pose estimation in both marker-based and markerless systems is achieved by using at least three noncollinear markers or landmarks to define the pose of body segments, which are represented by local coordinate systems (LCS) relative to a global coordinate system (GCS). To create these coordinate systems and subsequent joint centres in traditional marker-based motion analysis, specific anatomical landmarks

must be identified through expert physical palpation, a skill that necessitates knowledge of anatomy and the translation of this information to a specific individual. Lack of adequate skill or experience in this domain leads to the misrepresentation of anatomical landmarks and unrepresentative anatomical coordinate systems and subsequent joint centres, which propagate to errors in reported joint kinematics and kinetics (Della Croce et al., 1999; Holden and Stanhope, 1998; Stagni et al., 2000). This has been noted as one of the greatest sources of error in motion analysis, being greater than instrument error and similar to skin movement artefact (Della Croce et al., 2005). Systematic bias in landmarks for a given examiner may also exist which make the consolidation of different datasets and multi-center collaborations challenging (Gorton et al., 2009; Johnson et al., 2018).

In markerless systems of the type studied here, joint centers and other salient landmark positions are directly estimated on new data by a deep learning algorithm based on training the algorithm has received on a training dataset (Cronin, 2021; Drazan et al., 2021; Mathis et al., 2018). These landmark positions, which have associated probabilities

* Corresponding author at: Human Mobility Research Laboratory, Hotel Dieu Hospital, 166 Brock St, Kingston, ON K7L 5G2, Canada.

E-mail address: r.kanko@queensu.ca (R.M. Kanko).

that reflect the algorithm's confidence in each estimated position, are generated based only on the training the network received and the new data provided, thereby dissociating the tracking of human motion from the operator (Cronin, 2021; Mathis et al., 2018).

Reducing the reliance on physical markers increases the ease of collecting data (Kanko et al., 2021a), may have the potential to improve the reliability of data (Kanko et al., 2021a), and may expand the use of quantitative human movement data to instances where marker-based motion analysis is not feasible or impedes the research (Cronin et al., 2019; Hutchinson et al., 2019; Mündermann et al., 2006; Verheul et al., 2020). Despite the potential opportunities presented by markerless motion capture, it is crucial that differences in kinematic measurements obtained using this technology relative to standard marker-based systems are examined to provide context for their use (Cronin, 2021; Dragan et al., 2021), and for researchers and clinicians to recognize that markerless systems represent an important supplementary technology that may allow different research questions to be answered (Dragan et al., 2021).

The aim of this study was to compare full-body 3D kinematics of gait measured by a deep neural network-based markerless motion capture system to those measured by a marker-based motion capture system.

2. Methods

2.1. Markerless motion capture

Theia3D (Theia Markerless Inc., Kingston, ON, Canada) is a deep learning algorithm-based approach to markerless motion capture that uses synchronized video data to perform 3D human pose estimation (Kanko et al., 2021a, 2021b). The system utilizes deep convolutional neural networks which were trained on over 500,000 manually annotated digital images of humans in the wild to estimate the position of 51 salient features on humans in new images provided to the system. The training dataset does not include any images of the testing data collected in our laboratory to ensure its performance is not better for our testing data than data collected in other environments. Using this approach, the system estimates the 2D positions of these features for all humans that appear within synchronized and calibrated video data provided to the system, from which 3D position estimates can be obtained. An articulated multi-body model is scaled to fit the subject-specific landmarks positions in 3D space, and a multi-body optimization approach (inverse kinematic (IK)) is used to estimate the 3D pose of the subject throughout the recorded physical task. This markerless system has previously been shown to measure comparable spatiotemporal gait parameters to marker-based motion capture and a pressure-sensitive gait mat, and reliably measure gait kinematics across multiple sessions (Kanko et al., 2021a, 2021b).

2.2. Participants

A sample of thirty healthy, recreationally active individuals (15 male/15 female, mean (SD) age: 23.0 (3.5) years, height: 1.76 (0.09) m, mass: 69.2 (11.4) kg) were recruited to participate in this study at the Human Mobility Research Laboratory (Kingston, ON). Participants gave written informed consent, and this study was approved by the institutional ethics committee. Exclusion criteria included having any neuromuscular or musculoskeletal impairments that could prevent their performance of walking. Participants were provided with minimal, skin-tight clothing, and wore their personal athletic shoes. Retroreflective markers and tracking clusters were affixed to relevant anatomical landmarks and body segments (Kanko et al., 2021b).

2.3. Experimental setup and procedure

A marker-based camera system (seven Qualisys 3+ (Qualisys AB, Gothenburg, Sweden), 1.3-megapixel resolution motion capture

cameras) and a markerless camera system (eight Qualisys Miqus, 3-megapixel resolution video cameras) were positioned around an instrumented treadmill (Tandem Force-Sensing Treadmill, AMTI Inc., MA). Both camera systems were connected to a single instance of Qualisys Track Manager for synchronization and to allow them to be calibrated simultaneously, resulting in a single shared global reference frame. Both systems recorded at 85 Hz.

A static calibration trial for the marker-based motion capture data was collected with the subject standing on the treadmill; no static trial is required for the markerless system. Starting at an initial speed of 1.2 m/s, participants determined a comfortable self-selected walking speed by providing feedback to researchers. Participants acclimatized to the treadmill for two minutes before ten consecutive trials of four seconds were collected simultaneously using both camera systems.

2.4. Data analysis

Markerless motion capture video data were processed using *Theia3D* (v2021.1.0.1450), from which 4x4 pose matrices of each body segment were exported for analysis in Visual3D (C-Motion, USA) alongside the tracked marker trajectories from the marker-based motion capture. The *Theia3D* lower body kinematic chain was constrained to have six degrees-of-freedom (DOF) at the pelvis and three DOF at the hip, knee, and ankle. Two skeletal models were created in Visual3D; one that tracked the markerless pose matrices, which Visual3D created automatically when data from *Theia3D* was loaded, and a second that tracked the marker trajectories, which was manually defined. The marker-based model was defined to have identical joint constraints as those of the *Theia3D* IK model.

Kinematic measures including joint center positions, lower limb global segment angles relative to the global coordinate system, and lower limb joint angles were calculated using the Visual3D models. Joint center positions for the markerless system were extracted from the automatic Visual3D model and represent direct estimates of those positions from the deep learning algorithm. Joint center positions for the marker-based system were estimated using the midpoint between the medial and lateral malleoli markers for the ankles, the midpoint between the medial and lateral femoral epicondyles for the knees, regression equations implemented in Visual3D adapted from (Bell et al., 1990, 1989) for the hips, a point offset inferiorly by 5 cm from the superior acromion marker for the shoulders, the midpoint between the medial and lateral humeral epicondyles for the elbows, and the midpoint between the radial and ulnar styloid processes for the wrists. Global segment angles represent the components of the XYZ Cardan angle taken between the segment LCS and the laboratory GCS (defined as Z-Up and Y-Anterior); thus, the x-component represents rotation about the global x-axis, the z-component represents rotation about the axially aligned axis of the segment LCS, and the y-component represents rotation about the floating axis produced by the cross product of the latter with the former. Joint angles were calculated using a Cardan sequence equivalent to the Joint Coordinate System (Grood and Suntay, 1983).

Force-based gait events were used to obtain time-normalized gait cycles, all of which were included in the analysis except those with tracking issues in the data from either system, which were excluded for both systems; this ensured the kinematic measurements being compared between systems were for identical gait cycles. The time-normalized kinematic measurements were analyzed in MATLAB (MathWorks, Natick, MA) by directly comparing measurements for matching gait cycles between systems and were summarized as subject-average differences and average root-mean-square (RMS) differences across all subjects.

The simultaneous markerless and marker-based data collected on thirty participants during treadmill walking analyzed here were previously analyzed to compare spatiotemporal gait parameters from both motion capture systems (Kanko et al., 2021b). Data were independently analyzed for these two studies, and the current work differs from the

previous analysis in the version of *Theia3D* software used and how the gait events were determined.

3. Results

Data from all thirty subjects were included in the analysis, using an average of 37 gait cycles per subject (range 11 to 51). The majority of tracking issues that led to the exclusion of a gait cycle were found in the marker-based data. Only gait cycles that were measured with both systems were included. Example skeletal models from the two systems are overlaid in Fig. 1A for visual comparison, and the markerless skeletal model is shown overlaid on the original video data in Fig. 1B. Visually, there is substantial overlap between the two models, providing face validity that the pose estimates were similar between the two systems.

3.1. Joint center position estimates

The average 3D Euclidean distance between corresponding lower limb joints throughout the gait cycle across all subjects was 2.4 cm, 2.2 cm, and 3.6 cm, for the ankle, knee, and hip, respectively. The lower limb joint center position differences demonstrated some dependence on gait cycle phase, indicating that there are systematic differences in the estimates from both systems that are dependent on subject pose (Fig. 2). The average 3D Euclidean distance between corresponding upper limb joints throughout the gait cycle across all subjects was 2.1 cm, 2.4 cm, and 1.1 cm at the shoulder, elbow, and wrist, respectively. The upper limb joint center position estimates were less dependent on gait cycle phase than the lower limb joints, with less variable differences throughout the gait cycle (Fig. 3).

3.2. Global segment angles

Subject-average lower limb segment angles relative to the global coordinate system measured using both motion capture systems and the average difference between the measurements are shown in Fig. 4. The thigh and shank segments were found to have very similar global segment angles between the marker-based and markerless system for the x- and y-components, with average RMS differences of 0.9°-2.2°. The thigh and shank global segment angle z-components had greater

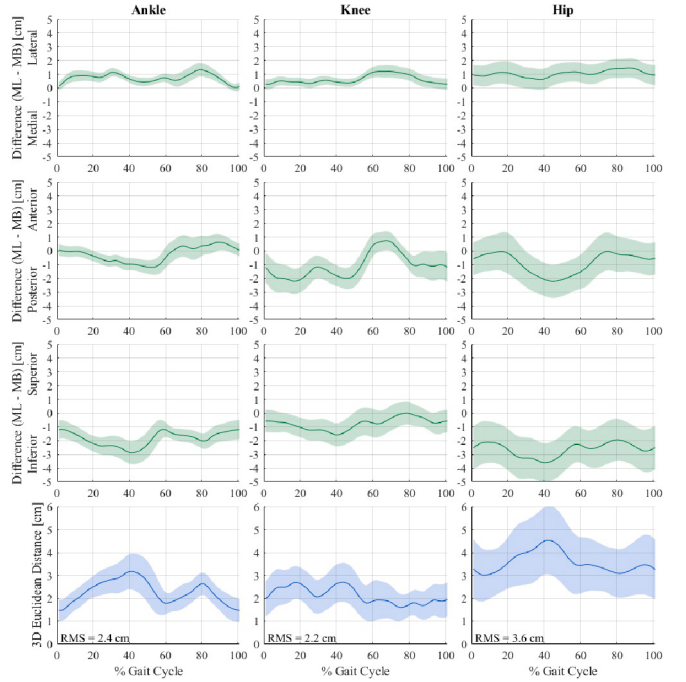


Fig. 2. Mean +/- SD lower limb joint position differences between both motion capture systems across the gait cycle for thirty subjects. Differences were calculated as [markerless (ML) position] - [marker-based (MB) position] and are expressed as components along each of the global coordinate system axes (row 1: medial/lateral direction; row 2: anterior/posterior direction; row 3: superior/inferior direction) and as 3D Euclidean distances (row 4). Axis labels (e.g. Lateral) indicate the position of the markerless joint relative to the marker-based joint. Root-mean-square (RMS) values are inset in the 3D Euclidean distance plots.

differences between the marker-based and markerless systems, of 8.5° and 13° respectively. The foot global segment angle x-components capture the greatest range of motion among the lower limb segments, and very similar patterns were measured by both systems across all

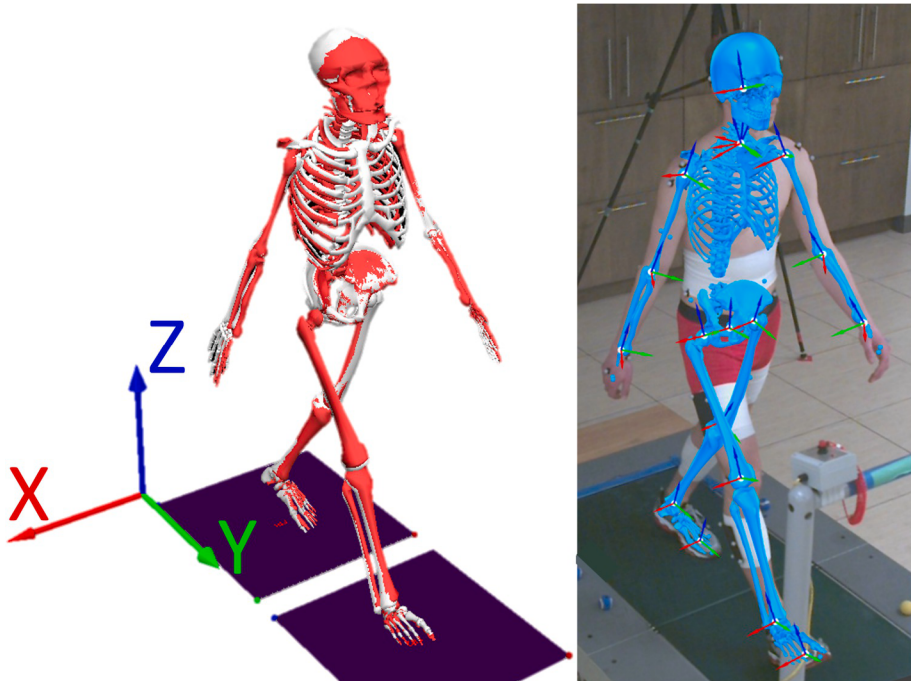


Fig. 1. Examples of A) the concurrent skeletal models with the global coordinate system, and B) the markerless skeletal model overlaid on original video data, with segment local coordinate systems displayed. The markerless skeletal model is shown coloured red in the image with the concurrent models, and coloured blue in the overlaid image. The global coordinate system is fixed in the treadmill, with the x-axis pointing laterally, the y-axis pointing in the direction of progression, and the z-axis pointing vertically. This subject had average joint position 3D differences at the ankle, knee, hip, shoulder, elbow, and wrist of 2.6 cm, 1.5 cm, 3.3 cm, 2.2 cm, 1.9 cm, and 1.1 cm, respectively. The joint angle RMS differences between the markerless and marker-based models for this subject were 10.1° in ankle flex/ext, 2.3° in knee flex/ext, 6.5° in hip flex/ext, 6.2° in ankle inv/ever, 3.6° in knee ab/ad, 2.1° in hip ab/ad, 9.8° in foot toe-in/out, 13.9° in knee int/ext rotation, and 3.1° in hip int/ext rotation angles.

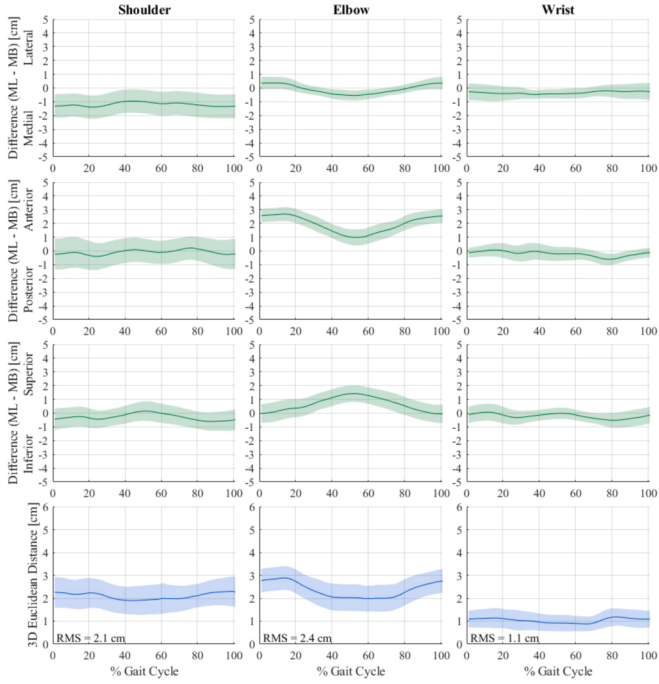


Fig. 3. Mean +/- SD upper limb joint position differences between both motion capture systems across the gait cycle for thirty subjects. Differences were calculated as [markerless (ML) position] - [marker-based (MB) position] and are expressed as components along each of the global coordinate system axes (row 1: medial/lateral direction; row 2: anterior/posterior direction; row 3: superior/inferior direction) and as 3D Euclidean distances (row 4). Axis labels (e.g. Lateral) indicate the position of the markerless joint relative to the marker-based joint. Root-mean-square (RMS) values are inset in the 3D Euclidean distance plots.

subjects, with an average RMS difference of 5.4° . The foot global segment angle y-components (similar to inversion/eversion) had greater differences between systems with an average RMS difference of 7.0° , while the z-components (similar to toe in/toe out) had little difference with an average RMS difference of 2.8° .

3.3. Lower limb joint angles

Subject-average lower limb joint angles measured using both motion capture systems are shown in Fig. 5, and lower limb joint angles for all cycles from one representative subject are shown in Fig. 6. Hip flexion/extension angles showed an offset between systems that decreased during early stance and at toe-off, which resulted in an average RMS difference of 11° . The ankle flexion/extension angles showed a similar but smaller offset that resulted in an average RMS difference of 6.7° . The knee flexion/extension angles demonstrated the greatest similarity among sagittal plane angles, with an average RMS difference of 3.3° . For all three joints, the marker-based system measured greater flexion than the markerless system.

The hip and knee ab/adduction joint angles showed high agreement between the marker-based and markerless systems, which had average RMS differences of 2.6° and 3.2° , respectively. The marker-based system typically measured greater knee adduction than the markerless system, particularly during swing phase (60–100% gait cycle). The ankle inversion/eversion angles had greater differences between systems, particularly during stance phase (10–50% gait cycle); the average RMS difference between systems for this angle was 8.0° .

The hip internal/external, knee internal/external, and foot toe-in/toe-out joint angles measured by the marker-based system had greater variability across all thirty subjects, whereas those waveforms from the markerless system were more similar across subjects. The internal/

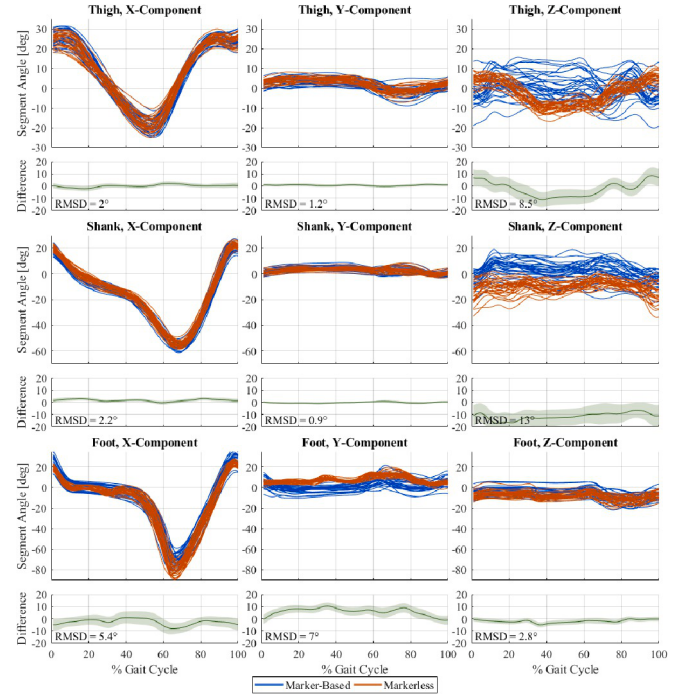


Fig. 4. Subject-average global segment angles of the thigh (row 1), shank (row 2), and foot (row 3) for thirty subjects measured by the markerless (orange) and marker-based (blue) motion capture systems, stacked above the average difference (markerless - marker-based) across all subjects. Segment angle x-components represent rotation about the laboratory GCS x-axis, z-components represent rotation about the axially aligned axis of the segment LCS, and y-components represent rotation about the floating axis produced by the cross product of the latter with the former. Average RMS differences are inset in each segment angle difference plot.

external hip rotation angles measured by the markerless system were more neutral than those from the marker-based system, and the average RMS difference between systems was 6.9° . The internal/external knee joint angles differed more during early stance and late swing phases, and the average RMS difference was 13.2° . The foot toe-in/toe-out angles measured by the markerless system follow a similar pattern to those measured by the marker-based system, but with less variability across subjects. The average RMS difference between the foot toe-in/toe-out angles was 11.6° .

4. Discussion

This study compared the kinematics of healthy adult treadmill gait measured by a marker-based motion capture system and a markerless motion capture system, finding comparable results between the two systems.

Across all thirty subjects, the joint center position estimates differed by less than 3 cm for all joints except the hip, which differed by 3.6 cm. These differences are similar in magnitude to the errors associated with different marker-based joint center location techniques which have been reported up to 4.59 cm for functional methods and 5.08 cm for predictive regression methods (Kainz et al., 2015). The lower limb joint center position differences were more sensitive to gait cycle phase compared to the upper limb joints, which may be a result of greater soft tissue artefacts for the lower limbs, less accurate markerless tracking due to occlusion by the treadmill safety bar (Fig. 1B), or blurred images due to the higher speeds at which the lower limbs travel during walking.

Both systems measured global segment angles with similar x-components, which capture the largest segment rotations during gait, differing by roughly 2° for the shank and thigh, and 5.4° for the foot.

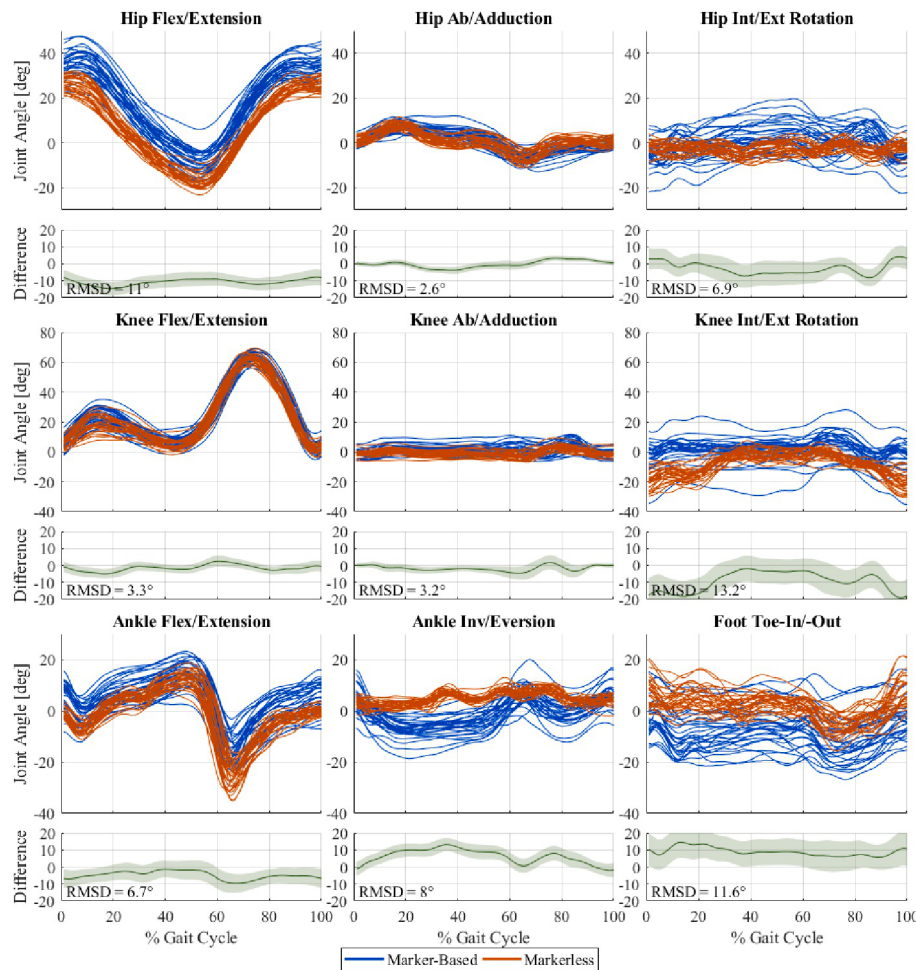


Fig. 5. Subject-average joint angles for the hip (row 1), knee (row 2), and ankle (row 3) for thirty subjects measured by the markerless (orange) and marker-based (blue) motion capture systems, stacked above the average difference (markerless - marker-based) across all subjects. Average RMS differences are inset in each joint angle difference plot.

Shank and thigh global segment angle y-components and foot global segment angle z-components had similarly small differences of less than 3° between systems. The largest segment angle differences were found for the foot segment y-component and the shank and thigh segment z-components, which are angular measurements taken about the LCS axis that is aligned with the segment long axis. In combination, the relatively small rotations of these segments about these axes and the alignment of the anatomical reference frames between the segments make these movements challenging for both systems to measure, resulting in greater differences of 7°–13°.

The lower limb joint angles captured similar patterns and ranges of motion in flexion/extension at the ankle, knee, and hip, and in ab/adduction at the knee and hip. Joint angles are measured between two adjacent body segments, and therefore any errors in global segment pose are amplified in these measurements. The offset in the ankle flex/extension angles is likely a result of the foot segment angle x-component differences, which had an average RMSD of 5.4°. Similarly, the offset in the hip flex/extension angles is likely a result of an offset in the pelvis segment poses between systems, since the differences in thigh segment angle x-components were small, with an average RMSD of 2.0°. Hip and knee internal/external rotation, foot toe-in/toe-out, and ankle inversion/eversion had the most apparent differences between the marker-based and markerless systems, with respect to both the waveform patterns captured and the variability among subjects. The larger differences observed in these joint angles are notable and challenging to interpret due to the likely presence of errors in the signals from both systems and

the lack of ground truth measurements.

There are several potential sources of error that could affect the measurements from both systems. Marker-based kinematics are susceptible to marker placement variation, kinematic crosstalk, soft tissue artefact, and joint center position regression errors. Inconsistent marker placement has been shown to contribute up to 5° of error in lower limb joint angles due to the procedure being performed by different operators and following different protocols (Gorton et al., 2009; Schwartz et al., 2004). To minimize this source of error, markers were placed by the same examiner across all subjects. It has also been shown that skin-mounted marker clusters move relative to the underlying bone during gait, with translations of up to 1.5 cm at the shank and 2.5 cm at the thigh, and rotations up to 8° (Benoit et al., 2015). These tissue artefacts introduce unpredictable, subject- and task-specific errors of up to 3° in knee joint angles (Benoit et al., 2015). Finally, joint center position estimation errors can also contribute up to 3° of error in lower limb joint kinematics (Kainz et al., 2015; Leboeuf et al., 2019).

Markerless kinematics may be affected by several factors associated with the markerless motion capture algorithm. The specific training of the neural networks used for automated pose estimation is both a strength and limitation of the markerless system. Any omissions or biases implicit within training datasets will be propagated to error when applied to situations where the training was weak. The sensitivity of the markerless motion capture system to various factors including subject characteristics such as age, sex, ethnicity, health status, anatomical deformities, and clothing have not yet been fully tested, nor has the

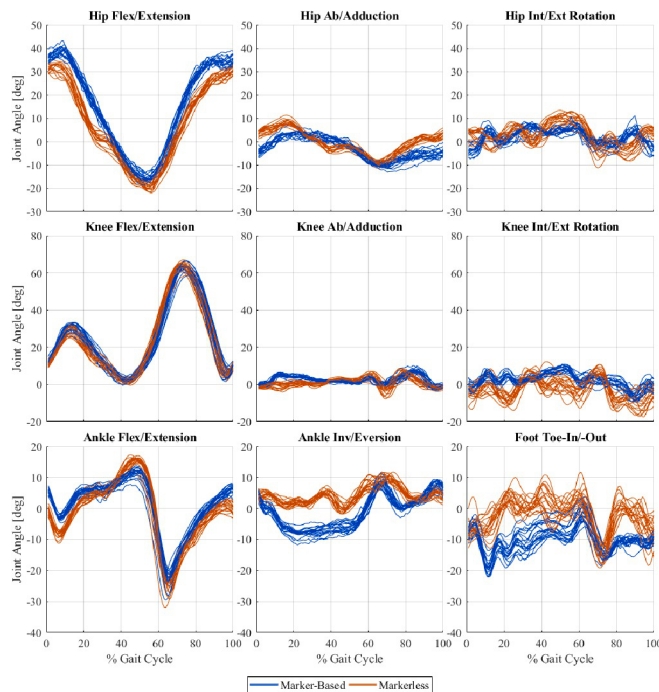


Fig. 6. Right lower limb joint angles for 19 gait cycles from one representative subject for the hip (row 1), knee (row 2), and ankle (row 3) measured by the markerless (orange) and marker-based (blue) motion capture systems.

sensitivity to environmental factors such as lighting or being in a laboratory. These potential sensitivities will require further testing since the results may differ for samples with different characteristics. The markerless system employs a frame-by-frame approach to track subject movement which may introduce greater noise to individual kinematic measurements compared to marker-based motion capture; however, previous work has indicated that this noise may be overcome by the use of multiple measurements (Kanko et al., 2021a) as is commonly done with marker-based motion capture. Additionally, this frame-by-frame approach may allow the system to be used to capture any visually observable task, regardless of whether the movement is typical or atypical, but this will require further testing to confirm.

Markerless kinematics may also be affected by several factors associated with the data collection, including occlusion by the treadmill safety bar (Fig. 1B), the unfamiliarity of the markerless system to motion capture markers and attire due to their absence from the training dataset, and suboptimal video data. The video cameras used were necessary for spatial and temporal synchronization with the marker-based system but were not ideal for the markerless system, producing images that were somewhat low resolution and blurry at times. Higher resolution video cameras, more light sensitive cameras, or increased ambient light would provide higher quality images and may improve tracking. Finally, this study examined treadmill gait, which is known to differ slightly from over-ground gait, so the results may differ for over-ground walking. However, since the markerless motion capture system uses a frame-by-frame approach to estimate pose and it has previously been tested on over-ground walking (Kanko et al., 2021a, 2021b), we believe that the differences would be minimal.

The results presented here indicate that joint center position and lower limb segment pose measurements were comparable between markerless and marker-based motion capture, except for segment axial rotations. Given the practical benefits of markerless motion capture such as minimal subject preparation time and reduced collection environment restrictions, this technology could allow studies to be undertaken with larger sample sizes than previously feasible. The similarity between the marker-based and markerless kinematics indicate that the

markerless system would be a suitable alternative technology in cases where the practical benefits of markerless data collection are preferred.

Declaration of Competing Interest

Scott Selbie is the CEO of Theia Markerless Inc. (Kingston, Ontario), the developers of Theia3D.

Acknowledgements

At the time of the study, RMK was supported by an NSERC Canadian Graduate Scholarship. We thank Human Mobility Research Laboratory members with participant recruitment, data collection, and data processing.

References

- Bell, A.L., Brand, R.A., Pedersen, D.R., 1989. Prediction of hip joint centre location from external landmarks. *Hum. Mov. Sci.* 8, 3–16. [https://doi.org/10.1016/0167-9457\(89\)90020-1](https://doi.org/10.1016/0167-9457(89)90020-1).
- Bell, A.L., Pedersen, D.R., Brand, R.A., 1990. A comparison of the accuracy of several hip center location prediction methods. *J. Biomech.* 23, 617–621. [https://doi.org/10.1016/0021-9290\(90\)90054-7](https://doi.org/10.1016/0021-9290(90)90054-7).
- Benoit, D.L., Damsgaard, M., Andersen, M.S., 2015. Surface marker cluster translation, rotation, scaling and deformation: Their contribution to soft tissue artefact and impact on knee joint kinematics. *J. Biomech.* 48, 2124–2129. <https://doi.org/10.1016/j.jbiomech.2015.02.050>.
- Cronin, N.J., 2021. Using deep neural networks for kinematic analysis: Challenges and opportunities. *J. Biomech.* 123, 110460 <https://doi.org/10.1016/j.jbiomech.2021.110460>.
- Cronin, N.J., Rantalaainen, T., Ahtialainen, J.P., Hyyninen, E., Waller, B., 2019. Markerless 2D kinematic analysis of underwater running: A deep learning approach. *J. Biomed. Eng.* 87, 75–82. <https://doi.org/10.1016/j.jbiomedech.2019.02.021>.
- Della Croce, U., Cappozzo, A., Kerrigan, D.C., 1999. Pelvis and lower limb anatomical landmark calibration precision and its propagation to bone geometry and joint angles. *Med. Biol. Eng. Comput.* 37, 155–161. <https://doi.org/10.1007/BF02513282>.
- Della Croce, U., Leardini, A., Chiari, L., Cappozzo, A., 2005. Human movement analysis using stereophotogrammetry: Part 4: assessment of anatomical landmark misplacement and its effects on joint kinematics. *Gait & Posture* 21, 226–237. <https://doi.org/10.1016/j.gaitpost.2004.05.003>.
- Drazan, J.F., Phillips, W.T., Seethapathi, N., Hullfish, T.J., Baxter, J.R., 2021. Moving outside the lab: markerless motion capture accurately quantifies sagittal plane kinematics during the vertical jump. *J. Biomech.* 110547 <https://doi.org/10.1016/j.jbiomech.2021.110547>.
- Gorton, G.E., Hebert, D.A., Gannotti, M.E., 2009. Assessment of the kinematic variability among 12 motion analysis laboratories. *Gait & Posture* 29, 398–402. <https://doi.org/10.1016/j.gaitpost.2008.10.060>.
- Grood, E.S., Sunay, W.J., 1983. A Joint Coordinate System for the Clinical Description of Three-Dimensional Motions: Application to the Knee. *J Biomed Eng* 105, 136–144. <https://doi.org/10.1115/1.3138397>.
- Holden, J.P., Stanhope, S.J., 1998. The effect of variation in knee center location estimates on net knee joint moments. *Gait & Posture* 7, 1–6. [https://doi.org/10.1016/S0966-6362\(97\)00026-X](https://doi.org/10.1016/S0966-6362(97)00026-X).
- Hutchinson, L.A., Brown, M.J., Deluzio, K.J., De Asha, A.R., 2019. Self-Selected walking speed increases when individuals are aware of being recorded. *Gait & Posture* 68, 78–80. <https://doi.org/10.1016/j.gaitpost.2018.11.016>.
- Johnson, W.R., Mian, A., Donnelly, C.J., Lloyd, D., Alderson, J., 2018. Predicting athlete ground reaction forces and moments from motion capture. *Med Biol Eng Comput* 56, 1781–1792. <https://doi.org/10.1007/s11517-018-1802-7>.
- Kainz, H., Carty, C.P., Modenese, L., Boyd, R.N., Lloyd, D.G., 2015. Estimation of the hip joint centre in human motion analysis: A systematic review. *Clin. Biomed. Eng.* 30, 319–329. <https://doi.org/10.1016/j.clinbiomech.2015.02.005>.
- Kanko, R.M., Laende, E., Selbie, W.S., Deluzio, K.J., 2021a. Inter-session repeatability of markerless motion capture gait kinematics. *J. Biomech.* 121, 110422 <https://doi.org/10.1016/j.jbiomech.2021.110422>.
- Kanko, R.M., Laende, E.K., Strutzenberger, G., Brown, M., Selbie, W.S., DePaul, V., Scott, S.H., Deluzio, K.J., 2021b. Assessment of spatiotemporal gait parameters using a deep learning algorithm-based markerless motion capture system. *J. Biomed. Eng.* 122, 110414 <https://doi.org/10.1016/j.jbiomech.2021.110414>.
- Leboeuf, F., Reay, J., Jones, R., Sangeux, M., 2019. The effect on conventional gait model kinematics and kinetics of hip joint centre equations in adult healthy gait. *J. Biomed. Eng.* 87, 167–171. <https://doi.org/10.1016/j.jbiomech.2019.02.010>.
- Mathis, A., Mamidanna, P., Cury, K.M., Abe, T., Murthy, V.N., Mathis, M.W., Bethge, M., 2018. DeepLabCut: markerless pose estimation of user-defined body parts with deep learning. *Nat. Neurosci.* 21, 1281. <https://doi.org/10.1038/s41593-018-0209-y>.
- Mündermann, L., Corazza, S., Andriacchi, T.P., 2006. The evolution of methods for the capture of human movement leading to markerless motion capture for biomechanical applications. *J. NeuroEng. Rehabil.* 3, 6. <https://doi.org/10.1118/1743-0003-3-6>.

- Schwartz, M.H., Trost, J.P., Wervey, R.A., 2004. Measurement and management of errors in quantitative gait data. *Gait & Posture* 20, 196–203. <https://doi.org/10.1016/j.gaitpost.2003.09.011>.
- Stagni, R., Leardini, A., Cappozzo, A., Grazia Benedetti, M., Cappello, A., 2000. Effects of hip joint centre mislocation on gait analysis results. *J. Biomech.* 33, 1479–1487. [https://doi.org/10.1016/S0021-9290\(00\)00093-2](https://doi.org/10.1016/S0021-9290(00)00093-2).
- Verheul, J., Nedergaard, N.J., Vanrenterghem, J., Robinson, M.A., 2020. Measuring biomechanical loads in team sports – from lab to field. *Science and Medicine in Football* 4, 246–252. <https://doi.org/10.1080/24733938.2019.1709654>.